HHS Public Access

Author manuscript

Mater Today Chem. Author manuscript; available in PMC 2019 June 01.

Published in final edited form as:

Mater Today Chem. 2018 June ; 8: 110–120. doi:10.1016/j.mtchem.2018.03.005.

Effects of PCL, PEG and PLGA polymers on curcumin release from calcium phosphate matrix for *in vitro* and *in vivo* bone regeneration

Susmita Bose[*], **Naboneeta Sarkar**, and **Dishary Banerjee**

W. M. Keck Biomedical Materials Research Laboratory, School of Mechanical and Materials Engineering, Washington State University, Pullman, Washington 99164, United States

Abstract

Calcium phosphate materials are widely used as bone-like scaffolds or coating for metallic hip and knee implants due to their excellent biocompatibility, compositional similarity to natural bone and controllable bioresorbability. Local delivery of drugs or osteogenic factors from scaffolds and implants are required over a desired period of time for an effectual treatment of various musculoskeletal disorders. Curcumin, an antioxidant and anti-inflammatory molecule, enhances osteoblastc activity in addition to its anti-osteoclastic activity. However, due to its poor solubility and high intestinal liver metabolism, it showed limited oral efficacy in various preclinical and clinical studies. To enhance its bioavailability and to provide higher release, we have used poly (ε-caprolactone) (PCL), poly ethylene glycol (PEG) and poly lactide co glycolide (PLGA) as the polymeric system to enable continuous release of curcumin from the hydroxyapatite matrix for 22 days. Additionally, curcumin was incorporated in plasma sprayed hydroxyapatite coated Ti6Al4V substrate to study *in vitro* cell material interaction using human fetal osteoblast (hFOB) cells for load bearing implants. MTT cell viability assay and morphological characterization by FESEM showed highest cell viability with samples coated with curcumin-PCL-PEG. Finally, 3D printed interconnected macro porous β-TCP scaffolds were prepared and curcumin-PCL-PEG was loaded to assess the effects of curcumin on *in vivo* bone regeneration. The presence of curcumin in TCP results in enhanced bone formation after 6 weeks. Complete mineralized bone formation increased from 29.6 % to 44.9% in curcumin-coated scaffolds compared to pure TCP. Results show that local release of curcumin can be designed for both load bearing or non-load bearing implants with the aid of polymers, which can be considered an excellent candidate for wound healing and tissue regeneration applications in bone tissue engineering.

Graphical Abstract

[*] sbose@wsu.edu, Phone: 509-335-7461.

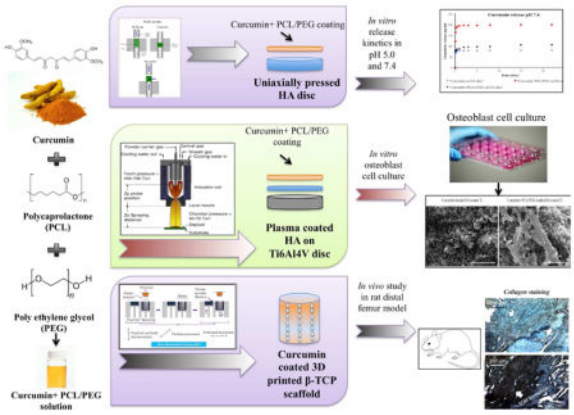

Keywords

Curcumin; 3D printing (3DP); Plasma coated Ti6Al4V; Osteoblast cell culture; *in vivo* osteogenesis

1. Introduction

Bone is a dynamic tissue with a unique capability of constant regeneration and reconstruction through the interaction of osteoblast, osteoclast and osteocyte, three kinds of living cells present in bone [1]. After a fracture, osteoblasts and osteocytes become active and promote osteogenesis or build bone and ultimately heal the injury. Osteoclasts, on the other hand, resorb old bone and helps in bone remodeling [2]. However, this self-healing ability of bone decreases with age and grafts become necessary for bone repair. Autograft harvesting includes risk of donor site morbidity, major vessel and visceral injuries, which leads to bleeding, chronic pain and hematoma. Moreover, many patients hesitate to agree upon a second surgery, which hinders the practical application of autograft. Allografts, on the other hand, not only produce immunogenic responses but also lack osteogenicity and osteoinductivity [3]. These drawbacks of autografts, allografts explain the development of artificial bone grafts for orthopedic applications utilizing calcium phosphate bioceramics, bioglass, polymers or metals as substrate [4].

Calcium phosphate ceramics, being the main inorganic component of bone, are widely used as scaffolds and metallic implant coating for bone tissue engineering to reconstruct, regenerate or enhance bone function [5]. They are also biocompatible and bioactive, which induces tissue ingrowth within the scaffold [6]. Among different phases of calcium phosphates, hydroxyapatite (HA) and β tricalcium phosphate (β-TCP) are intensively studied as bone substitutes due to their excellent osteoconductivity and strong binding ability with the host bone tissue. Various *in vitro* and *in vivo* drug delivery study has been conducted in which HA is exploited in various forms such as nanoparticles, coatings or porous scaffolds that promote attachment, proliferation and differentiation of bone cells [7–8].

In our quest for small natural regulators of osteogenesis, we have found that curcumin, the main active component derived from the rhizomes of turmeric plant (*Curcuma longa* L.) is one of the most extensively studied natural compounds due to its multiple therapeutic activities and medicinal properties [9]. Various clinical and pre-clinical reports exhibited that curcumin possess anti-inflammatory, anti-microbial, anti-oxidant, anti-arthritic, wound healing, and anti-carcinogenic properties [10–12]. Several *in vivo* and *in vitro* results show that curcumin has great potential against various types of human cancer, including leukemia, melanoma, breast cancer, colon cancer, pancreatic cancer, prostrate cancer, ovarian cancer etc [13–16]. At the cellular level, curcumin regulates many molecular targets including various transcription factors such as nuclear factor-κβ (NF-κβ), growth factors like TGF-β1 (tumor growth factor -β1), VEGF (vascular endothelial growth factor), and cytokines as IL1, IL2 (interleukin) and TNF-α (tumor necrosis factor-α). [17] Among them, NF-κβ is involved in bone remodeling process, which insinuates that curcumin may have possible effects on skeletal system [18]. Oral administration of curcumin inhibits osteoclast induced bone matrix degradation in insulin-dependent diabetic rat model [19]. It also prevented osteoclastogenesis by inhibiting NF-κβ in RAW 264.7 cells [20]. Another study showed 50% decreased proliferation of MG-63 osteosarcoma cells but 80% increased viability of healthy osteoblast cells after treating with 10 μm curcumin [21].

However, poor bioavailability of curcumin due to low serum concentration, limited tissue absorption, high metabolic rate, and rapid elimination from body hinders its practical application [22]. Researchers have developed various novel formulations such as nanoparticles, liposomes, micelles, phospholipid complexes, implants etc. to improve absorption, biodistribution, metabolism and elimination of curcumin [23]. Local or targeted drug delivery system, such as implants bypasses the oral route and delivers the drug directly to the systemic circulation, enhancing bioavailability [24]. In this study, we administered a highly water-soluble polymer, poly ethylene glycol (PEG) to alleviate poor tissue adsorption and rapid metabolism. Poly ethylene glycol is an extensively studied hydrophilic polymer composed of repeating units of hydrophilic ethylene oxide (—CH2—CH2—O—) monomers. PEG has been used in numerous drug-delivering vehicles and tissue engineering application because of its solubility in both organic and hydrophilic solvents. PEG, even at a low concentration, forms a protective, dense, hydrophilic cloud of long flexible chains and thus lowers the surface hydrophobicity of the drug molecule. Increasing surface hydrophilicity also allows for cell adhesion and proliferation on biomaterial scaffolds by preventing protein adsorption, a process by which proteins denature and adhere to the outer layer of biomaterials *in vivo* [25–26]. Additionally, polycaprolactone (PCL) or poly-lactide co glycolide (PLGA) is incorporated to maintain continuous release of curcumin from the scaffold at the implantation site. PCL and PLGA are FDA-approved, biocompatible and biodegradable polymers, widely used in tissue engineering scaffolds for sustained and controlled delivery of drugs, proteins and other macromolecules [27–28]. Our objective is successful fabrication of curcumin loaded calcium phosphate scaffolds, which can effectively be used as local drug delivery system for enhanced osteogenesis in various skeletal disorders or bone-regeneration application.

To promote cell proliferation, extracellular matrix deposition, and vascularization, a scaffold must possess highly porous structure with interconnected porosity [29]. An average pore

size of 200–400 μm is desired in a bone tissue-engineering scaffold to promote bone growth [30]. Among a variety of processing methods for synthesizing porous bone scaffolds, 3D printing technology has the advantage of faster processing of scaffolds with designed porosity from a CAD file, without the need for specific tool or dies [31]. 3D printed HA and TCP scaffolds with interconnected macro and micro pores were prepared to mimic highly porous nature of natural bone. This scaffold showed no toxicity, adequate *in vitro* cell adhesion and *in vivo* biocompatibility as well as new bone formation at the implant-bone interface and inside the interconnected pores [32]. However, low mechanical property of this porous ceramic scaffolds restrict its practical applications only in low-load or non-load bearing implants (Table 1).

For load bearing hip and knee implants, metallic substrates with HA coating are extensively used since the last four decades [33]. Metallic implants, being poor osteoconductors does not promote bone growth within the implant and forms fibrous tissue encapsulation, which leads to loosening of implant [34]. To improve bone bonding with the metallic implants, the surface of the metal substrate is coated with HA ceramics [35]. Among a variety of coating techniques, plasma spray is most popular due to ease of operation, low cost, low substrate temperature and higher deposition rate. Induction plasma spray, an electrode free system, is beneficial for synthesizing high purity HA coating, which eliminates the chances of contamination from electrode [36].

Very few studies revealed that curcumin might have the ability to regulate bone remodeling. Most of the research articles have studied effects of curcumin by using it as dietary supplements or incorporating drug solution directly to the cell culture system. There are no studies on *in vitro-in vivo* release kinetics of curcumin from porous or dense calcium phosphate scaffolds for bone tissue engineering. In this report, *in vitro* release study was performed to assess the effects of PLGA-PEG and PCL-PEG on release kinetics of curcumin. Our aim was to formulate improved release of curcumin in both phosphate and acetate buffer medium. After we received promising drug release from the hydroxyapatite matrix, our goal was to study *in vitro* osteoblast cell (hFOB) proliferation on curcumin loaded HA plasma coated Ti64 substrate for load bearing application. To observe the effect on bone in growth, 3D printed interconnected porous TCP scaffolds were synthesized and impact of polymeric curcumin was assessed by *in vivo* bone regeneration. We hypothesize that coating of PCL-PEG and PLGA-PEG polymers would alter the release of curcumin from the calcium phosphate matrix, improve the *in vitro* osteoblast cell proliferation and attachment and enhance the bone and blood vessel formation *in vivo*.

2. Material and Methods

2.1 In vitro curcumin release kinetics study

2.1.1 Scaffold preparation—HA powders (Monsanto, USA) were mixed with ethanol in (2:3 W/V ratio) and ball milled for 12 hours with zirconia balls (ball:powder ratio is 3:1). After milling, ethanol was evaporated by keeping it in conventional oven at 60°C overnight. Dried powders were obtained which were sieved to get uniform particle size and then pressed into disk (12 mm diameter and 2 mm thickness) using an uniaxial press. For each disc, 0.6 g of powder was measured, put into cylindrical molds and a uniaxial pressure of

165 MPa was applied for 2 minutes. Green scaffolds were obtained which were sintered in a conventional muffle furnace at 1250 °C for 2 h.

2.1.2 Drug-polymer coating—Drug solution was prepared by dissolving 0.25 g of curcumin in 20 ml of ethanol. Two different polymer solutions were prepared. One with polycaprolactone (PCL) and polyethylene glycol (PEG) in 65:35 ratio and another with poly-lactide co glycolide (PLGA) and PEG in 65:35 ratio [37]. We went through a series of optimization steps to select the workable ratio for PCL and PEG. After the initial investigation of different polymer ratio (100% PCL, PCL:PEG 65:35, PCL:PEG 50:50, PCL:PEG 35:65 and 100% PEG), we observed that presence of PEG (8K) (35% w/w) along with PCL (65% w/w) controlled the drug release in the initial burst phase and improved release in later phase, leading to a desired release Presence of 100% PCL and PCL:PEG 65:35 exhibited undesirable slow release of curcumin, whereas 100% PEG, PCL:PEG 50:50 showed initial burst release of curcumin. Each of the polymer mix was dissolved in 5 ml of dichloromethane (DCM), making two different polymer solutions. 10ml of drug solution is added and mixed with the 5 ml polymer solution. Therefore the concentration of curcumin in final drug-polymer solution becomes 0.125g in 15 ml. 30 μl of drug-polymer solution was added on top of both surfaces of the HA discs so that the total drug amount reached to 500 μg in each discs. Finally, the solvents were evaporated at room temperature by keeping the samples in the dark overnight.

2.1.3 In Vitro curcumin release—Curcumin release study was investigated in both pH 7.4 phosphate buffer and pH 5.0 acetate buffer. The 7.4 pH is used to imitate physiological pH, whereas 5.0 pH resembles the post-surgery acidic micro-environment. The pH range is kept within ±0.05 using a pH probe. Samples in triplicate were placed in 4 mL of buffer solution. Then they are kept at a shaker at 37 °C under 150 rpm of constant shaking. The buffer solutions were changed at each time point and replaced with freshly prepared 4 mL buffer solution. The concentration of curcumin was determined using Biotek Synergy 2 SLFPTAD microplate reader (Biotek, Winooski, VT, USA). The absorbance values were obtained at 425 nm wavelength and drug concentration was calculated using a normal plot.

2.1.4 Dissolution, and surface morphology after release—Field emission scanning electron microscope (FESEM) (FEI Inc., Hillsboro, OR, USA) was used to characterize surface morphologies of all scaffolds to observe phase dissolution after release. Before performing FESEM, the scaffolds are left to dry at room temperature for 72 hours. Then, they were gold coated using a sputter-coater (Technics Hummer V, CA, USA).

2.2 In vitro osteoblast cell culture study

2.2.1 Scaffold preparation—20 mm thick, grade 5, Ti6Al4V substrate (Titanium Joe, Canada) were sandblasted and cut by water jet to form disc shaped samples with 12.5 mm diameter. The samples are then ultrasonicated with DI water and acetone. As received HA powder (Monsanto, USA) of about 400–500 μm is used for coating. An inductively coupled RF plasma spray system (Tekna Plasma Systems, Canada) (30 kW) equipped with axial powder feeding system was used to coat the HA powder on Ti6Al4V substrate. 25 kW plate power, 110 mm working distance and a supersonic plasma nozzle is used for this study.

Argon (Ar) with flow rate of 25 and 13 standard liters per minute (slpm) was used as the central and carrier gas. A mixture of 60 slpm Ar and 6 slpm hydrogen (H_2) was used as sheath gas. The chamber pressure was kept at 5 pound-force per square inch gauge (psig). All these parameters were optimized in previous study [30].

2.2.2 Osteoblast cell culture—Prior to cell culture, all samples were sterilized by autoclaving at 121 °C for 60 min. Human osteoblast cell line hFOB (PromoCell GmbH, Germany) were used for this culture. Samples were kept in 24 well plates and cells were seeded onto the samples at a density of 2×10^6 cells/mL. Osteoblast growth medium (PromoCell GmbH, Germany) was used to maintain the culture for the entire study. Cultures were kept in an incubator at 37°C under an atmosphere of 5% CO_2 as recommended by PromoCell for this particular cell line. Growth medium was changed every 2 days during the entire cell culture study.

2.2.3 Cell morphology—To characterize cellular morphology by FESEM, samples were separated from culture after 3,7 and 11 days of study. The samples were fixed with 2% paraformaldehyde/2% glutaraldehyde in 0.1M cacodylate buffer overnight at 4 °C. 2% osmium tetroxide (OsO_4) is used for post-fixation for 2 h at room temperature. Then, the samples were dehydrated in a series of ethanol (30%, 50%, 70%, 95% and 100% three times), followed by hexamethyldisilane (HMDS) drying. Samples are kept in a vacuum desiccator for overnight drying. Gold coating with thickness of 10–15 nm was applied using a gold sputter coater. The morphology of samples are then studied using FESEM (FEI 200F, FEI Inc., OR, USA).

2.2.4 MTT cell viability assay—Osteoblast (hFOB) cell viability was evaluated using MTT (3-(4,5-dimethylthiazol-2-yl)-2,5-diphenyl tetrazolium bromide) (Sigma, St. Louis, MO) assay. To prepare MTT solution, 5 mg of MTT is dissolved in 1 ml of sterile filtered PBS. 100 μl of MTT solution was then added to each sample in 24-well plates followed by addition of 900 μl of cell medium. The samples were incubated for 2 h. 1 ml of MTT solubilizer is prepared using 10% Triton X-100, 0.1N HCl and isopropanol. After incubation, 600 μl of MTT solubilizer was added to dissolve the formazan crystals. Thereafter, 100 μl of that solution was transferred into a 96-well plate, and read by UV–Vis spectroscopy microplate reader (BioTek) at 570 nm. To ensure reproducibility, all samples were used in triplicate. Data are presented as mean ± standard deviation. Student's t-test was used to perform statistical analyses and P values < 0.05 and <0.0001 are considered significant and extremely significant.

2.3 In Vivo study

2.3.1 Scaffold preparation—Solid-state synthesis process was used to prepare pure β-TCP powder. Briefly, 1 M calcium carbonate ($CaCO_3$) is mixed with 2 M calcium phosphate dibasic ($CaHPO_4$) and ball milling was carried out for 2 hour to achieve homogeneous mixing with media: powder ratio maintained at 4:1. Thereafter calcination is done at 1050°C for 24 hrs. The powder is sieved and then ball-milled with 2:3 W/V ethanol (200 proof, Decon Labs, PA) for 6 h using 5:1 ball and powder ratio. The solvent was driven off at 60°C in a conventional furnace by keeping it overnight. Cylindrical scaffolds of 3.2 mm diameter

and 5 mm height along with 3D interconnected pores with pore size of 400 μm was designed where the square shaped pores penetrates orthogonally through the cylinder in X, Y and Z directions. 3D printer (ProMetal®, ExOne LLC, Irwin, PA, USA) was used to fabricate these designed scaffolds. The aqueous binder used for 3D printing was purchased from ProMetal®, ExOne LLC, Irwin, PA, USA. Thereafter, the binder were cured at 175°C for 90 min to form a green scaffold. Loosely adhered powder clogged within the pores was removed by air blowing. These scaffolds were then sintered at 1250°C (sintering cycle: 3°C/min to heating rate up to 120°C, then 3°C/min heating rate up to 600°C, 1 hour dwell time, and then 1°C/min heating rate up to 1250°C, 2 hour dwell time, 10°C/min cooling rate) in a conventional muffle furnace for 2 hour.

2.3.2 Drug-Polymer Coating—Curcumin was dissolved in anhydrous ethanol at a concentration of 1mg/ml. Polymer solution is prepared by mixing PCL and PEG in 65:35 molar ratio and dissolving the mixture in anhydrous ethanol at 5 wt%. 50 μl of drug-polymer solution were pipetted onto the entire scaffolds to achieve desired drug loading.

2.3.3 Pore size and coating morphology—FESEM was performed to calculate pore size as well as to characterize surface morphologies of the scaffolds. Prior to FESEM, the samples were gold coated using a sputter-coater. Pore size was calculated by taking an average measurement from three scaffolds.

2.3.4 Surgery and implantation procedure—Sprague-Dawley rats (Charles Rivers Laboratories International, Inc., Wilmington, MA, USA) with 280–320 g of body weight were used in this study. A protocol approved by Institutional Animal Care and Use Committee (IACUC), Washington State University was obeyed while performing the surgeries. The rats were kept in temperature and humidity controlled rooms with alternate cycles of 12 h dark and 12 h light. After the animals get acclimated, surgery was performed to generate a femoral defect. Anesthesia was carried out by using IsoFlo® (isoflurane, USP, Abbott Laboratories, North Chicago, IL, USA) along with oxygen (Oxygen USP, A-L Compressed Gases Inc., Spokane, WA, USA). Pedal reflex and respiration rate of the rats were monitored to maintain proper surgical anesthesia. The 3/5 mm defect was created in the distal femur bone by making a through and through hole using a drill bit of 2/3 mm diameter. Physiological saline was used to cleanse the cavity and remove the remaining bone fragments present in the defect site. Thereafter drug-polymer coated TCP scaffolds were press fitted at the defect site. Pure TCP scaffolds were used as control. To close the wound an absorbable synthetic surgical suture, undyed braided-coated VICRYL polyglactin 910 (Ethicon Inc., Somerville, NJ, USA), was used. Betadine solution as a disinfectant was applied at the wound site to prevent post surgery infection. Meloxical injection was applied to reduce the pain after the surgery. Rats were euthanized by CO_2 overdose after 6 weeks post-surgery. The bone-implant specimens were cut from the rat body using a rotating saw and then fixed with 10% neutral buffered formalin solution for 72 hours.

2.3.5 Histomorphology and histomorphometric analysis by Modified Masson Goldner's trichrome (Undecalcified tissue sections)—A series of dehydration process is carried out for the bone tissue specimens using ethanol (70%, 95% and 100%),

ethanol:acetone (1:1) and 100% acetone. Each step is carried out for 8–12 hours. Now, the specimen is kept in acetone: spurrs resin (2:1 and then 1:1) for infiltration. Next, the sample tube/vial is filled with acetone:spurrs resin (1:1) and kept overnight with the lid open so the acetone evaporates. Then, 100% spurs resin is used to keep the tissue specimens. Lastly, bone-implant specimen is kept in a mold filled with 100% spurrs resin at 60°C overnight. After the samples is embedded in spurrs resin, a thin section of 200 μm is cut with the help of slow speed diamond saw cutter and attached on a glass slide using super glue. After drying the slide, the tissue sections were stained by Masson Goldner's trichrome stain and observed under optical microscope [Olympus BH-2, Olympus America Inc., USA].

Histomorphometric analysis is carried out using ImageJ software (NIH) to measure percentage fraction of newly formed bone area (area covered by newly formed bone/area of the entire tissue section, %). 1/1 mm tissue sections was used to measure the newly formed bone area (n=6).

2.3.6 Histomorphology by collagen, vWf and H&E staining (Decalcified tissue sections)—The formalin fixed tissue samples were washed with DI water 2–3 times and then kept in 14% EDTA solution for at least 8–12 weeks for decalcification. The EDTA solution is changed in every 2 days. When the specimen is completely decalcified, it is rinsed with DI water four times. Dehydration process is carried out by keeping the specimen in series of ethanol (30%, 50%, 70% and 100%), xylene-ethanol (1:1) and 100% xylene. After this, the specimen is kept in 1:1 xylene:paraffin and kept at 60°C for overnight. Lastly, the specimen is embedded in 100% paraffin. 5–15 μm tissue sections were cut using a diamond saw cutter and deparaffined by keeping it in a water bath at about 40–45°C. Then the tissue-implant specimen is placed on the positively charged slide so that it gets attached to the slide by electrostatic interactions. After drying the slides, collagen, vWf and H&E staining was carried out. Fig. 2 shows a schematic of the *in vitro* and *in vivo* experimental procedure.

3. Results

3.1 In vitro drug release and surface morphology

Fig. 3 shows curcumin release profiles from HA discs coated with, a) only curcumin b) PCL-PEG curcumin (c) PLGA-PEG curcumin in the phosphate buffer. Curcumin being a hydrophobic drug showed very low release from the hydroxyapatite matrix. After 22 days time point, it showed only 16% release of total drug loading, after which it achieved the plateu range. Curcumin has metal ion chelating ability; this ensures that curcumin adheres to the matrix by binding to the calcium ions present in the HA. This can be another reason for low release of curcumin. Whereas, addition of PEG and PCL made the drug hydrophilic and showed much higher release due to better aqueous solubility. It exhibited 39% of drug release in the first 24 hours. PLGA-PEG co polymer system, on the other hand, showed a more lower drug release. Therefore, after 22 days time point, 21% of drug has been released. Higher drug release in case of PCL can be attributed to the fact that dissolution rate decreases with increased polymer molecular weight.

Fig. 4 shows cumulative release profiles of curcumin from HA discs coated with, a) only curcumin b) PCL-PEG curcumin (c) PLGA-PEG curcumin at acetate buffer. Similar trend is observed in pH 5.0, apart from the fact that an overall higher release of curcumin can be seen in pH 5.0 than pH 7.4. The increased stability of curcumin in acidic pH condition may be contributed by the conjugated diene structure. Curcumin showed very low release and achieved a plateau range. After 22 days, 23% drug has been released. In case of PCL-PEG co polymer system, very high release of curcumin can be seen. 61% of drug was released in the first 24 hours. After 22 days time point, 64% of drug was released and it went to a plateau range. In case of PLGA-PEG co polymer system, curcumin is showing much more lower release. After 22 days time point, 26 % of total curcumin has been released and has reached the plateau range.

Fig. 5 shows surface morphologies of pure HA+ curcumin, pure HA + curcumin+ PCL/PEG and pure HA + curcumin + PLGA/PEG at pH 5.0 and 7.4 after 22 days release. Much less surface degradation is observed at pH 7.4 than pH 5.0. The samples kept in acidic pH clearly showed much higher degradation, which is evident from the rough and inhomogeneous HA surface. This result is in accordance to the release kinetics of curcumin in acidic pH. This high porosity is attributed to the higher release of the curcumin from the matrix.

3.2 In vitro osteoblast cell proliferation and morphology

Fig. 6 shows SEM images of osteoblast cell culture of day 3, day 7 and day 11 on vitamin C loaded HA coated Ti samples. Curcumin, being hydrophobic, showed very low release from HA matrix. Therefore it could not show its effect on osteoblast proliferation as we can compare with the control. Addition of PCL/PEG and PLGA/PEG make curcumin hydrophilic and therefore its remarkable effect on osteoblast cell proliferation can be observed, as compared to control. Day 11 PCL/PEG-CURC and PLGA/PEG-CURC samples show apatite formation on osteoblast cells.

Figure 7 shows osteoblast (hFOB) cell viability of pure and curcumin coated samples after day 3,7 and 11 by MTT assay. Presence of PCL/PEG along with curcumin shows highest osteoblast cell density in all time points compared to all other samples. Presence of PLGA/PEG showed slightly increase in cell viability in day 3 and day 11, compared to control and only curcumin-coated samples. However, it is interesting to note that curcumin without presence of polymer releases in a very low amount from matrix and therefore does not exhibit any pronounced effect on osteoblast cell viability compared to control samples.

3.3 In vivo scaffold morphology and histomorphological characterization

Figure 8 shows surface morphology of 3D printed pure and curcumin coated TCP scaffolds after sintering. Interconnected designed porosity is observed in both control TCP and curcumin coated TCP scaffolds with pore size reaching around 340–350 μm after sintering. As we know, during densification, pores present in the scaffold shrink, resulting in smaller pore size after sintering. Apart from the designed porosity, some intrinsic residual micropores of about 10–15 μm are also present in uniform manner in all the samples. However, presence of PCL-PEG-Curcumin coating on the 3D printed scaffold did not alter the surface morphology as seen from the microstructure.

Figure 9(a) depicts histomorphological characterization by modified Masson Goldner trichrome staining after 6 weeks to show effect of curcumin+PCL-PEG coating on new bone formation. The image taken by optical microscope can be interpreted as reddish orange color resembling osteoid like new bone formation and greenish for mineralized bone or collagen. Curcumin+PCL-PEG coated TCP scaffold shows a prominent increase in osteoid formation and mineralization of the newly formed bone as compared to the control TCP scaffold. The new bone formation is already initiated inside the macro pores of the implant and host bone interface site after 6 weeks of surgery suggesting pronounced effect of curcumin+PCL-PEG coating on enhanced osteoid formation and osseointegration. Figure 9(b) shows histomorphometric analysis by ImageJ software showing enhanced osteoid like new bone formation in curcumin coated TCP scaffolds compared to control TCP scaffolds.

Figure 10 shows histomorphology of implant-tissue sections by collagen, von Willebrand Factor (vWF) and Hematoxylin & Eosin (H&E) staining showing osteogenesis and angiogenesis after 6 weeks of surgery. The collagen staining kit is basically composed of specific mouse monoclonal antibody, which identifies various species of type II collagen present in articular hyaline cartilage of rat. The dark region shows presence of type II collagen, which marks the formation of extracellular matrix. Presence of curcumin +PCL/PEG shows distinctive ECM formation compared to control samples with no curcumin. vWf is a glycoprotein produced by endothelial cells and therefore widely used to show new blood vessel formation, enhanced vascularity and angiogenesis. Dark brown region shown in curcumin+PCL-PEG coated TCP scaffolds resembles blood vessel formation as compared to the bare TCP scaffolds with no such region, implying lack of blood vessel formation. There are purple regions, which clearly signifies presence of nuclei. Therefore, presence of curcumin+PCL-PEG shows enhanced angiogenesis in the implant-tissue interface, which is preferred in early wound healing after a surgery. H&E staining is performed to show osteoid like new bone formation in pink color, blood vessel formation by dark red and nuclei can be seen in dark blue/purple color. The histomorphological sections of curcumin+PCL/PEG show not only new bone formation but also enhanced vascularization in tissue-implant interface compared to the bare TCP scaffold.

4. Discussion

Curcumin being water-insoluble, exhibits rapid metabolism and elimination, which hinders its *in vivo* practical applications. Numerous investigations have been carried out to improve bioavailability of cucrumin using various biodegradable polymers like PEG, PLGA and PCL. PEG is a polymer exploited for its excellent aqueous solubility, flexible polymer chain and low toxicity [38,25]. Even at a low concentration, PEG forms a protective, dense, hydrophilic cloud of long flexible chains and thus lowers the surface hydrophobicity of the drug molecule. PCL [39,27] and PLGA [40,28], on the other hand, were added to control the burst release of curcumin in the first few hours. We have reported in our previous studies that a thin layer of PCL coating exhibited controlled drug release behavior. PLGA is FDA approved, extensively studied biodegradable and biocompatible polymer used for sustained and controlled drug delivery from implant.

Local delivery of curcumin from bone tissue engineering scaffolds, avoid the disadvantages of oral drug delivery process, such as need for high drug dosage because of the poorly irrigated bone tissue. Reports showed 40-fold increase of bioavailability of curcumin using PLGA compared to curcumin without polymer [41]. Compared to aqueous solution of curcumin, PLGA-PEG formulation was reported to increase the bioavailability by 55.4 fold [42]. PLGA with 50:50 ratio of PLA/PGA, exhibit degradation at about two months due to hydrolysis of the ester linkages [43]. However, pronounced difference has not been shown in PLGA-PEG curcumin samples compared to conventional curcumin coated samples. PCL has been extensively used as polymeric coating for bone tissue engineering scaffolds to show controlled protein and drug release kinetics, compared to uncoated samples. PCL/PEG-curcumin samples showed much enhanced drug release in the aqueous environment. We attributed this behavior to the high molecular weight of PLGA (~45000) than PCL (~14000). Dissolution rate of polymer decreases with increased polymer weight [44].

After we received promising drug release from dense HA matrix with the aid of polymer system, we studied its effect on *in vitro* bone forming cells, i.e human fetal osteoblast cells. Previous reports presented that curcumin downregulates NF–κβ-signaling pathway, activation of which suppresses osteoblast differentiation and stimulates osteoclastic bone resorption. Curcumin prohibits phosphorylation and degradation of NF–κβ inhibitor (Iκβ). As a result, transcription factor, NF–κβ remains conjugated with Iκβ. NF–κβ-Iκβ complex being unable to enter nucleus, stays inactive within the cytoplasm [45]. Curcumin also suppresses TNF-α, a cytokine, found in elevated amount in post-menopausal women and associated with the postmenopausal osteoporosis [46]. These results support *in vitro* osteoblast MTT assay as well as the SEM images, where higher amount of osteoblast cell viability and proliferation has been observed with curcumin-PCL/PEG samples.

The SEM images and MTT cell viability assay is in accordance to the *in vitro* release kinetics data. Presence of PCL/PEG and PLGA/PEG co-polymer system increases hydrophilicity of curcumin and allow the drug to release in the medium. Curcumin, after getting released from the scaffold, interacts with osteoblast and enhances the cell viability, which supports our hypothesis. Whereas, only curcumin, being hydrophobic, trapped within the HA coating cannot get released in the medium. Therefore, it does not show much pronounced effect on cell viability except in day 11.

Dense scaffolds and coated implants are not ideal to show bone in growth due to their significantly low porosity. To observe *in vivo* bone regeneration within the pores, scaffolds must have optimum porosity [29–30]. The 3D printing technique allows fabrication of ideal bone tissue engineering scaffolds featuring interconnected pores with multiscale porosity [47]. In the present paper, we have processed bioresorbable CaP scaffold with designed macropores (340–350 μm), which play an important role in cell and ion transport. Additionally, presence of micropores of about 10–15 μm increases the surface area for protein adsorption, provides area for osteoblast attachment and thereby improves bone ingrowth within scaffolds. Interconnected pores are important for vascularization, which transports nutrients to the cells and removes waste products [48]. After successful fabrication of scaffolds with complex geometry, they can be utilized to deliver various biomolecules with osteogenic and angiogenic properties.

Bone has self-healing ability. However, it takes several months to completely heal a fracture. Incorporation of biomolecules, growth factors, or dopants often shortens this healing time and thus helps in early recovery of patient. Osteoblasts are the cells, which helps in the formation of new bone. Osteoid is the un-mineralized bone matrix (often referred to 'new bone'), which is formed by osteoblasts cells, prior to the maturation of bone tissue. Osteoblast starts the bone formation process by secreting osteoid in the forms of various bone proteins. Therefore, a biomolecule like curcumin, which can positively influence osteoblast proliferation, should show faster osteoid formation or early wound healing. The polymers used in this study (PCL, PEG and PLGA) are FDA approved and shows no toxicity or adverse effects towards bone tissue and therefore have been chosen by many researchers as a potential candidate for bone tissue engineering applications. [25–28,38–40]

Modified masson goldner trichrome staining clearly distinguishes osteoid like new bone formation, stained red, and from matured bone matrix, stained green. Osteoid is unmineralized bone matrix secreted by bone forming osteoblast cells, which, after calcification, turns into mineralized bone tissue [49]. Results show bone mineralization was not complete in control TCP, whereas complete mineralization and osseointegration was observed in curcumin coated TCP after 6 weeks. Though type I collagen is abundant in extracellular matrix of bone, articular hyaline cartilage (articular surface of bone) is mainly composed of type II collagen (80–85%) [50]. Therefore, histological evaluation of collagen II formation provided valuable information about bone healing after implantation. Results show considerable amount of ECM formation took place in the samples containing curcumin compared to the control. A study reported enhanced synthesis, deposition, maturation and cross linking of collagen occurred at the damaged tissue of rats due to the presence of curcumin. Angiogenesis or blood vessel formation is important for tissue ingrowth as they provide nutrients and oxygen to individual cells. vWf staining showed enhanced formation of blood vessel in curcumin-PCL-PEG coated scaffolds compared to control. In HE staining, amount of osteoid formation within the scaffold can be easily identified. The white spots in control sample shows the scaffold area, which implies lack of osteogenesis in the defect site. However, curcumin-PCL/PEG coated samples displayed osteoid formation, angiogenesis as well as several nuclei, which gave us a general overview on the status of the bone growth and wound healing.

Conclusion

In this study, *in vitro* curcumin release from HA matrix has been improved by using polymers. Addition of PCL-PEG and PLGA-PEG co polymer system enhance its bioavailability as well as improved its release from the porous calcium phosphate ceramics. Load bearing plasma coated HA on Ti6Al4V substrate was fabricated to assess osteoblast proliferation in presence of curcumin. MTT assay and FESEM show significant enhancement in osteoblast cell viability by Curcumin+PCL-PEG coated scaffolds compared to control samples. 3D printing was utilized to fabricate pure and curcumin coated TCP scaffolds for non-load bearing tissue engineering application with designed porosity of 500 μms. The presence of curcumin in TCP on early wound healing was clearly demonstrated by enhanced bone formation after 6 weeks compared to control TCP scaffolds. Complete mineralized bone formation increased from 29.6 % to 44.9% in curcumin-coated scaffolds

compared to pure TCP. Thus, interconnected macro porous 3DP curcumin coated TCP scaffolds can be considered as an excellent candidate for wound healing and tissue regeneration applications in bone tissue engineering.

Supplementary Material

Refer to Web version on PubMed Central for supplementary material.

Acknowledgments

Researchers would like to acknowledge help from Washington Animal Disease Diagnostic Lab (WADDL) and financial assistance from NIH [Grant # 1R01-AR-066361].

References

1. Hadjidakis DJ, Androulakis II. Bone remodeling. Annals of the New York Academy of Sciences. 2006
2. Moore WR, Graves SE, Bain GI. Synthetic bone graft substitutes. ANZ J Surg. 2001; 71(6):354–361. [PubMed: 11409021]
3. Kneser U, et al. Tissue engineering of bone: the reconstructive surgeon's point of view. Journal of cellular and molecular medicine. 2006; 10(1):7–19. [PubMed: 16563218]
4. LeGeros RZ, Lin S, Rohanizadeh R, Mijares D, LeGeros JP. Biphasic calcium phosphate bioceramics: preparation, properties and applications. J Mater Sci Mater Med. 2003; 14(3):201–209. [PubMed: 15348465]
5. Bose S, Tarafder S. Calcium phosphate ceramic systems in growth factor and drug delivery for bone tissue engineering: a review. Acta Biomater. 2012; 8(4):1401–1421. [PubMed: 22127225]
6. de Groot K. Bioceramics of calcium phosphate. CRC; 1983.
7. Bose S, Roy M, Bandyopadhyay A. Recent advances in bone tissue engineering scaffolds. Trends Biotechnol. 2012; 30(10):546–554. [PubMed: 22939815]
8. Shor L, Güçeri S, Wen X, Gandhi M, Sun W. Fabrication of three-dimensional polycaprolactone/hydroxyapatite tissue scaffolds and osteoblast-scaffold interactions in vitro. Biomaterials. 2007; 28(35):5291–5297. [PubMed: 17884162]
9. Maheshwari RK, Singh AK, Gaddipati J, Srimal RC. Multiple biological activities of curcumin: a short review. Life sciences. 2006; 78(18):2081–2087. [PubMed: 16413584]
10. Anand P, Thomas SG, Kunnumakkara AB, Sundaram C, Harikumar KB, Sung B, Tharakan ST, Misra K, Priyadarsini IK, Rajasekharan KN, Aggarwal BB. Biological activities of curcumin and its analogues (Congeners) made by man and Mother Nature. Biochem Pharmacol. 2008; 76(11): 1590–1611. [PubMed: 18775680]
11. Menon VP, Sudheer AR. The molecular targets and therapeutic uses of curcumin in health and disease. Springer US; 2007. Antioxidant and anti-inflammatory properties of curcumin; 105–125.
12. Basniwal RK, Buttar HS, Jain VK, Jain N. Curcumin nanoparticles: preparation, characterization, and antimicrobial study. J Agric Food Chem. 2011; 59(5):2056–2061. [PubMed: 21322563]
13. Odot J, Albert P, Carlier A, Tarpin M, Devy J, Madoulet C. In vitro and in vivo anti-tumoral effect of curcumin against melanoma cells. Int J Cancer. 2004; 111(3):381–387. [PubMed: 15221965]
14. Aggarwal BB, Shishodia S, Takada Y, Banerjee S, Newman RA, Bueso-Ramos CE, Price JE. Curcumin suppresses the paclitaxel-induced nuclear factor-κB pathway in breast cancer cells and inhibits lung metastasis of human breast cancer in nude mice. Clin Cancer Res. 2005; 11(20): 7490–7498. [PubMed: 16243823]
15. Dhillon N, Aggarwal BB, Newman RA, Wolff RA, Kunnumakkara AB, Abbruzzese JL, Ng CS, Badmaev V, Kurzrock R. Phase II trial of curcumin in patients with advanced pancreatic cancer. Clin Cancer Res. 2008; 14(14):4491–4499. [PubMed: 18628464]

16. Kuo M, Huang T, Lin J. Curcumin, an antioxidant and anti-tumor promoter, induces apoptosis in human leukemia cells. Biochimica et Biophysica Acta (BBA)-Molecular Basis of Disease. 1996; 1317(2):95–100. [PubMed: 8950193]
17. Aggarwal BB, Sung B. Pharmacological basis for the role of curcumin in chronic diseases: an age-old spice with modern targets. Trends Pharmacol Sci. 2009; 30(2):85–94. [PubMed: 19110321]
18. Rohanizadeh R, Deng Y, Verron E. Therapeutic actions of curcumin in bone disorders. Bonekey Rep. 2016; 5
19. French DL, Muir JM, Webber CE. The ovariectomized, mature rat model of postmenopausal osteoporosis: an assessment of the bone sparing effects of curcumin. Phytomedicine. 2008; 15(12): 1069–1078. [PubMed: 18693096]
20. Oh S, Kyung T, Choi H. Curcumin Inhibits Osteoclastogenesis by Decreasing Receptor Activator of Nuclear Factor-κB Ligand (RANKL) in Bone Marrow Stromal Cells. Molecules & Cells (Springer Science & Business Media BV). 2008; 26(5)
21. Chang R, Sun L, Webster TJ. Selective cytotoxicity of curcumin on osteosarcoma cells compared to healthy osteoblasts. Int J Nanomedicine. 2014; 9:461. [PubMed: 24453488]
22. Anand P, Kunnumakkara AB, Newman RA, Aggarwal BB. Bioavailability of curcumin: problems and promises. Mol Pharm. 2007; 4(6):807–818. [PubMed: 17999464]
23. Prasad S, Tyagi AK, Aggarwal BB. Recent developments in delivery, bioavailability, absorption and metabolism of curcumin: the golden pigment from golden spice. Cancer Res Treat. 2014; 46(1):2. [PubMed: 24520218]
24. Sun DongmeiZhuang XiaoyingXiang XiaoyuLiu YuelongZhang ShuangyinLiu CunrenBarnes StephenGrizzle WilliamMiller DonaldZhang Huang-Ge. A novel nanoparticle drug delivery system: the anti-inflammatory activity of curcumin is enhanced when encapsulated in exosomes. Mol Ther. 2010; 18(9):1606–1614. [PubMed: 20571541]
25. D'souza Anisha A, Shegokar Ranjita. Polyethylene glycol (PEG): a versatile polymer for pharmaceutical applications. Expert opinion on drug delivery. 2016; 13(9):1257–1275. [PubMed: 27116988]
26. FanunMonzer, editorsColloids in drug delivery. Vol. 150. CRC Press; 2016.
27. Williams JM, Adewunmi A, Schek RM, Flanagan CL, Krebsbach PH, Feinberg SE, Hollister SJ, Das S. Bone tissue engineering using polycaprolactone scaffolds fabricated via selective laser sintering. Biomaterials. 2005; 26(23):4817–4827. [PubMed: 15763261]
28. Jain Rajeev A. The manufacturing techniques of various drug loaded biodegradable poly (lactide-co-glycolide)(PLGA) devices. Biomaterials. 2000; 21(23):2475–2490. [PubMed: 11055295]
29. Mastrogiacomo M, Scaglione S, Martinetti R, Dolcini L, Beltrame F, Cancedda R, Quarto R. Role of scaffold internal structure on in vivo bone formation in macroporous calcium phosphate bioceramics. Biomaterials. 2006; 27(17):3230–3237. [PubMed: 16488007]
30. Gauthier O, Bouler JM, Aguado E, Pilet P, Daculsi G. Macroporous biphasic calcium phosphate ceramics: influence of macropore diameter and macroporosity percentage on bone ingrowth. Biomaterials. 1998; 19(1):133–139. [PubMed: 9678860]
31. Bose S, Vahabzadeh S, Bandyopadhyay A. Bone tissue engineering using 3D printing. Mater Today. 2013; 16(12):496–504.
32. Bose SusmitaTarafder SolaimanBandyopadhyay Amit. Effect of chemistry on osteogenesis and angiogenesis towards bone tissue engineering using 3D printed scaffolds. Annals of biomedical engineering. 2017; 45(1):261–272. [PubMed: 27287311]
33. De Groot K, Wolke JGC, Jansen JA. Calcium phosphate coatings for medical implants. Proc Inst Mech Eng H J Eng Med. 1998; 212(2):137–147.
34. Roy M, Bandyopadhyay A, Bose S. Induction plasma sprayed nano hydroxyapatite coatings on titanium for orthopaedic and dental implants. Surf Coat Technol. 2011; 205(8):2785–2792. [PubMed: 21552358]
35. Filiaggi MJ, Coombs NA, Pilliar RM. Characterization of the interface in the plasma-sprayed HA coating/Ti-6Al-4V implant system. J Biomed Mater Res. 1991; 25(10):1211–1229. [PubMed: 1667401]

36. Vahabzadeh Sahar, et al. Phase stability and biological property evaluation of plasma sprayed hydroxyapatite coatings for orthopedic and dental applications. Acta biomaterialia. 2015; 17:47–55. [PubMed: 25638672]
37. Bansal Shyam S, Vadhanam Manicka V, Gupta Ramesh C. Development and in vitro-in vivo evaluation of polymeric implants for continuous systemic delivery of curcumin. Pharmaceutical research. 2011; 28(5):1121–1130. [PubMed: 21311958]
38. Gref R, et al. The controlled intravenous delivery of drugs using PEG-coated sterically stabilized nanospheres. Advanced drug delivery reviews. 2012; 64:316–326.
39. Tarafder S, Bose S. Polycaprolactone-coated 3D printed tricalcium phosphate scaffolds for bone tissue engineering: in vitro alendronate release behavior and local delivery effect on in vivo osteogenesis. ACS Appl Mater Interfaces. 2014; 6(13):9955–9965. [PubMed: 24826838]
40. Makadia Hirenkumar K, Siegel Steven J. Poly lactic-co-glycolic acid (PLGA) as biodegradable controlled drug delivery carrier. Polymers. 2011; 3(3):1377–1397. [PubMed: 22577513]
41. Lee WH, Loo CY, Young PM, Traini D, Mason RS, Rohanizadeh R. Recent advances in curcumin nanoformulation for cancer therapy. Expert opin drug deliv. 2014; 11(8):1183–1201. [PubMed: 24857605]
42. Khalil NM, do Nascimento TCF, Casa DM, Dalmolin LF, de Mattos AC, Hoss I, Romano MA, Mainardes RM. Pharmacokinetics of curcumin-loaded PLGA and PLGA–PEG blend nanoparticles after oral administration in rats. Colloids Surf B: Biointerfaces. 2013; 101:353–360. [PubMed: 23010041]
43. Gentile P, Chiono V, Carmagnola I, Hatton PV. An overview of poly (lactic-co-glycolic) acid (PLGA)-based biomaterials for bone tissue engineering. Int J Mol Sci. 2014; 15(3):3640–3659. [PubMed: 24590126]
44. Miller-Chou Beth A, Koenig Jack L. A review of polymer dissolution. Progress in Polymer Science. 2003; 28(8):1223–1270.
45. Plummer SM, Holloway KA, Manson MM, Munks RJ, Kaptein A, Farrow S, Howells L. Inhibition of cyclo-oxygenase 2 expression in colon cells by the chemopreventive agent curcumin involves inhibition of NF-kB activation via the NIK/IKK signalling complex. Oncogene. 1999; 18(44): 6013–6020. [PubMed: 10557090]
46. Xu YX, Pindolia KR, Janakiraman N, Chapman RA, Gautam SC. Curcumin inhibits IL1 alpha and TNF-alpha induction of AP-1 and NF-kB DNA-binding activity in bone marrow stromal cells. Hematopathol Mol Hematol. 1997; 11(1):49–62. [PubMed: 9439980]
47. Tarafder S, Balla VK, Davies NM, Bandyopadhyay A, Bose S. Microwave-sintered 3D printed tricalcium phosphate scaffolds for bone tissue engineering. J Tissue Eng Regen Med. 2013; 7(8): 631–641. [PubMed: 22396130]
48. Kalfas Iain H. Principles of bone healing. Neurosurgical focus. 2001; 10(4):1–4.
49. Gruber HE. Adaptations of Goldner's Masson trichrome stain for the study of undecalcified plastic embedded bone. Biotech Histochem. 1992; 67(1):30–34. [PubMed: 1617000]
50. Junqueira LCU, Cossermelli W, Brentani R. Differential staining of collagens type I, II and III by Sirius Red and polarization microscopy. Arch Histol Japon. 1978; 41(3):267–274.

Highlights

- *In vitro* curcumin release from porous calcium phosphate ceramics has been improved by the addition of PCL-PEG and PLGA-PEG co polymer system.
- MTT cell viability assay and morphological characterization by FESEM after 3, 7 and 11 days showed highest osteoblast cell viability and proliferation in HA plasma coated Ti6Al4V samples with presence of curcumin-PCL-PEG compared to control samples without curcumin.
- 3D printing was utilized to fabricate TCP scaffolds with designed porosity of 500 μms and was coated with curcumin-PCL-PEG to understand its effects on *in vivo* bone regeneration.
- After six weeks, complete mineralized bone formation increased from 29.6 % to 44.9% in curcumin-coated scaffolds compared to control showing excellent early wound healing and osteogenesis ability by curcumin.

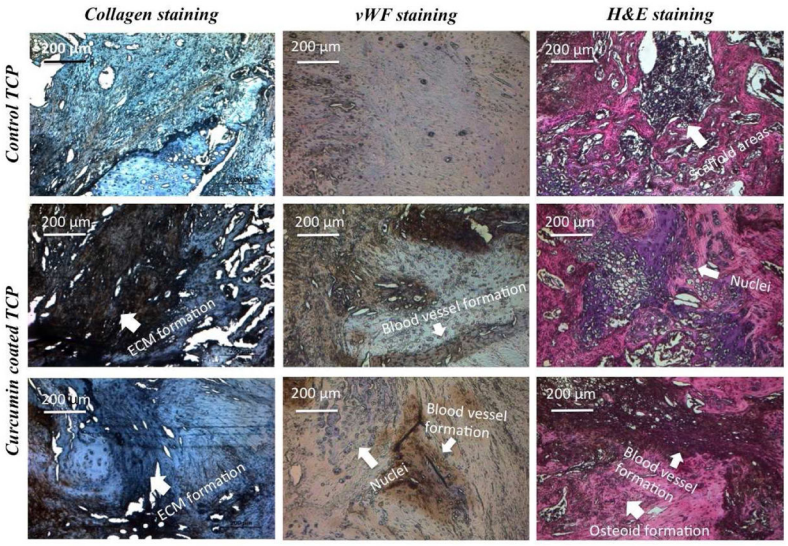

Fig. 2.

Schematic representation of experimental procedure of *in vitro* release kinetics and *in vivo* study in rat distal femur model

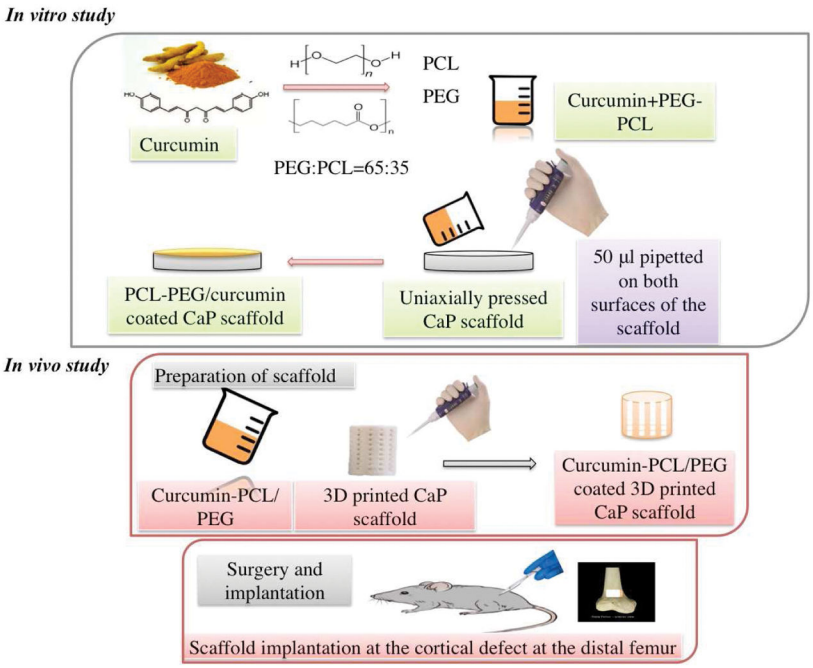

Fig. 3.

Curcumin release profiles from HA discs coated with, a) only curcumin b) PCL-PEG curcumin (c) PLGA-PEG curcumin at pH 7.4 (inset shows the initial burst release in first 24 hours). Curcumin release increased to 39% in first 24 hours with the addition of polymers compared to without polymer.

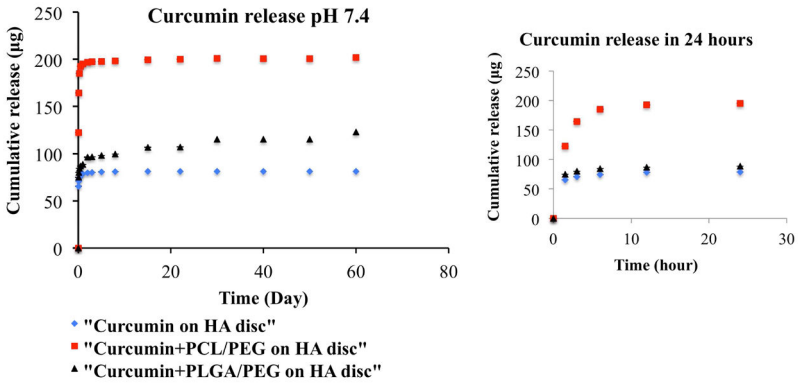

Fig. 4.

Curcumin release profiles from HA discs coated with, a) only curcumin b) PCL-PEG curcumin (c) PLGA-PEG curcumin at pH 5.0 (inset shows the initial burst release in first 24 hours). 64% of total drug was released with the addition of PCL-PEG polymer system compared to without polymer.

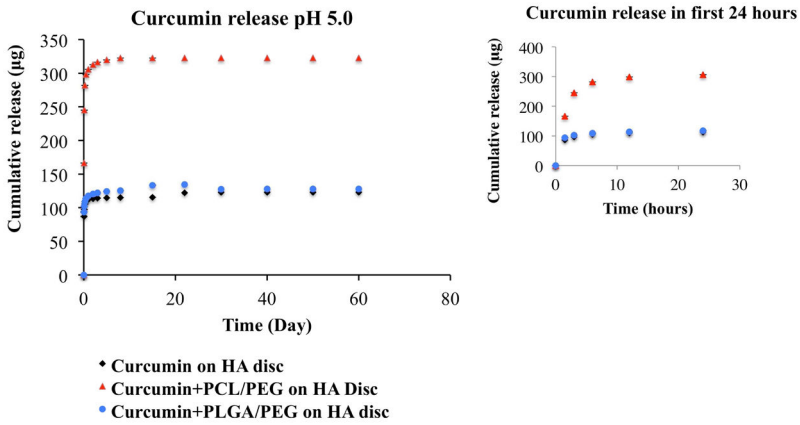

Fig. 5.

Surface morphologies of pure HA+ curcumin, pure HA + curcumin+ PCL/PEG and pure HA + curcumin + PLGA/PEG at pH 5.0 and 7.4 after 22 days release. Higher surface degradation in pH 5.0 than pH 7.4 results in increased curcumin release from the matrix

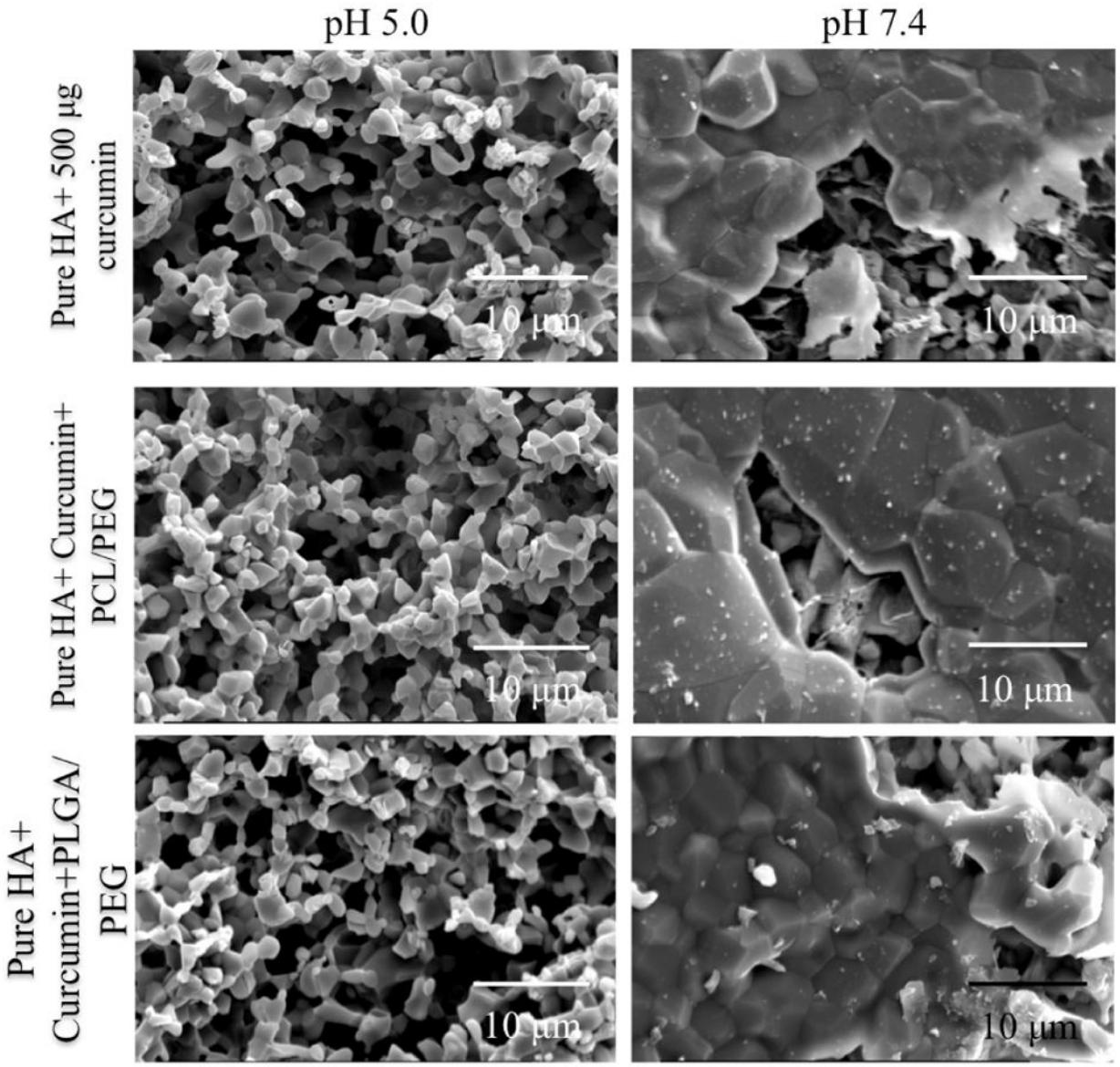

Fig. 6.

SEM images for osteoblast cell culture of pure, pure+curcumin, pure+curcumin+PCL/PEG, pure+curcumin+PLGA/PEG samples after day 3,7 and 11 days of culture. Regardless of the time point, polymeric curcumin coated samples exhibiting much higher cell proliferation compared to samples without polymer.

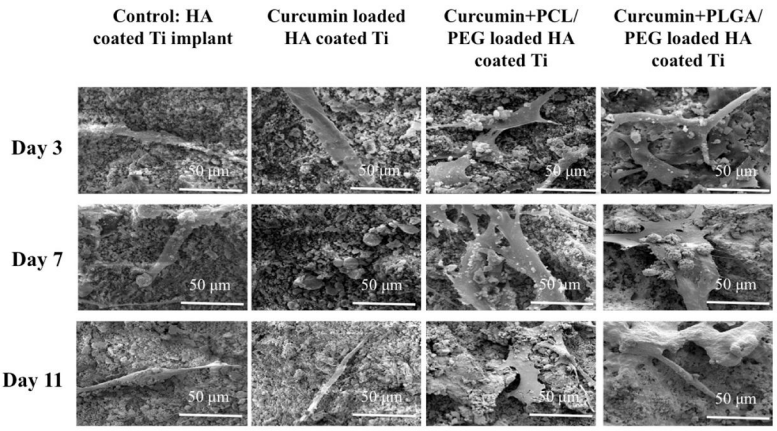

Fig. 7.

Osteoblast (hFOB) cell viability of pure, pure+curcumin, pure+curcumin+PCL/PEG, pure +curcumin+PLGA/PEG samples after day 3,7 and 11 days of culture by MTT assay (n=9). * denote P values < 0.0001, extremely statistically significant, ** denote P values <0.05, statistically significant, ***denote P value > 0.05, not statistically significant. Curcumin with PCL-PEG showing statistically extremely significant difference compared to samples without polymer.

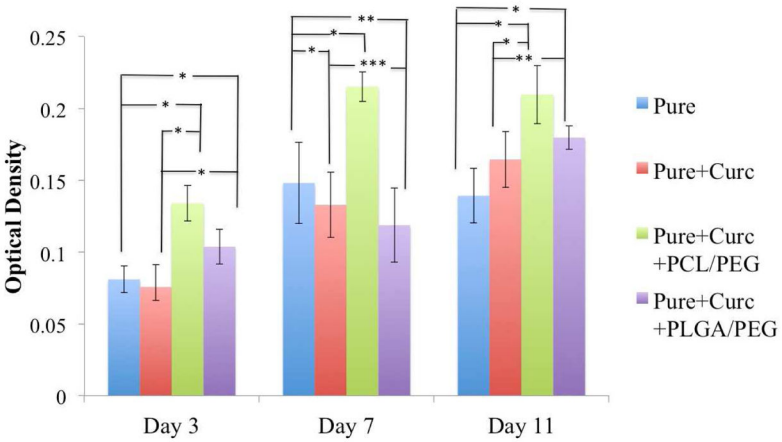

Fig. 8.

Surface morphology of pure and curcumin coated TCP scaffolds. Measured pores after sintering are 340 to 350 μm.

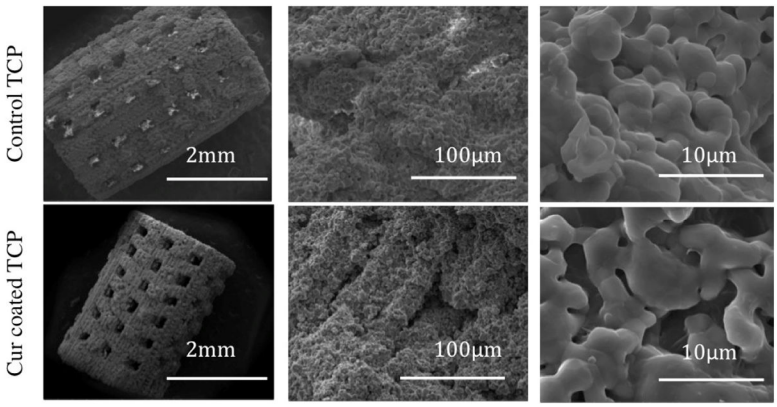

Fig. 9.

(a) Optical microscopy images of tissue-implant sections after modified Masson Goldner trichrome staining showing osteoid like new bone formation in reddish orange color and mineralized bone in greenish color, (b) Histomorphometric analysis by ImageJ showing percentage of osteoid formation.

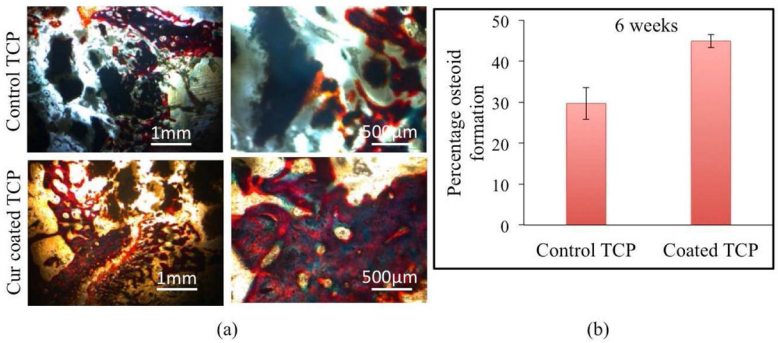

Fig. 10.

Optical microscopy images of decalcified tissue-implant specimens after collagen, von Willebrand Factor (vWF) and Hematoxylin & Eosin (H&E) staining showing extracellular matrix formation, angiogenesis and osteoid formation respectively after 6 weeks of surgery in rat distal femur model

Table 1

Mechanical properties of HA coated Ti implant and 3D printed TCP scaffold (n=5)

Mechanical Properties		
HA coated Ti implant	Bond strength	17.4±2.9 MPa
3D printed TCP scaffold	Compressive strength test	6.7±1.1 MPa